Computational hair quality categorization in lower magnifications

Computational hair quality categorization in lower magnifications

Barmak Heshmat[a*], Hayato Ikoma[a], Ik Hyun Lee[a], Krishna Rastogi[a,b], Ramesh Raskar[a]
[a]Media Lab, Massachusetts Institute of Technology, Cambridge, MA, USA
[b]PES Institute of Technology, Bangalore, Karnataka, India

ABSTRACT

We take advantage of human hair specific geometry to visualize sparse submicron cuticle peelings with highly oblique tip-side illumination. We show that the statistics of these features can directly estimate hair quality in much lower magnifications (down to 20×) with less powerful objectives when the features themselves are below the system resolution. Our technique for quality categorization of black, blond, and grey human scalp hair samples is successful in all cases. This technique has strong potential for lower cost, portable, and autonomous hair diagnostic apparatuses.

Keywords: dark field microscopy, oblique illumination microscopy, portable diagnostics, human hair

1. INTRODUCTIONS

Hair quality can be detected with conventional polarimetry techniques, SEM and different spectroscopic techniques[1-9]. Hair quality can be classified thoroughly by extensive spectroscopy and analysis of the essential components in hair down to molecular level. The current instruments for analyzing hair quality are rather bulky and relatively expensive[5-9]. Additionally, it is not always necessary to analyze the chemical compounds of hair as the effects of some of the invasive factors are manifested in the geometry of the hair[4, 9]. Unfortunately the variations in the features of the cuticles of healthy and unhealthy (UV damaged[9]) hair are rather small (submicron) in *x-y* plane (sample plane) and close to diffraction limit of optical microscopy. These are three dimensional features that can have larger *z* variation that is not necessarily visible in a simple widefield microscopy configuration. Therefore, higher magnification objectives with large numerical aperture (e.g. 100× with 1.4NA) and more complex interferometric or confocal techniques are necessary to study these features[2, 3, 5, 6]. This higher resolution is obtained in price of reduced field of view and depth of field, increased alignment sensitivity and complexity. Other challenges for using optical microscopy while studying human hair is the absorption and scattering of light by inner structures of hair (cortex and medulla) in black hair (Fig. 1 (a)) in transmission mode and strong reflection of light from outer layers in blonde or grey hair (Fig. 1 (b)) in reflection mode.

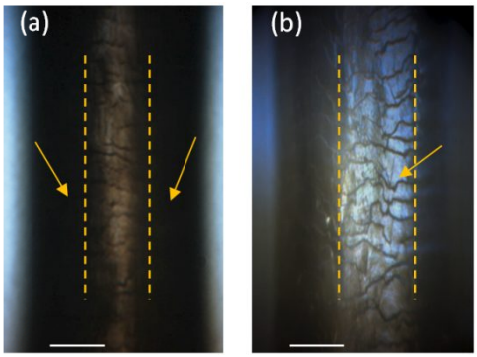

Figure 1. Challenges in using conventional illumination configurations with low magnification objective (20× 0.75NA) (a) Black hair is imaged in transmission mode. Absorption and scattering from inner layers reduces the signal to noise ratio (SNR) at the areas shown by arrows. (b) The intense reflection in the middle region (shown by arrow) from the outer layers and the geometry of the hair renders the sides of the blonde hair dark. This requires larger dynamic range sensor. Scale bars are 40 micrometer.

We have taken the idea of oblique illumination[10] to extreme. Here we have employed near perpendicular (highly oblique illumination) to capture microscopic images of hair for extracting mechanical damage features. By exploiting the

Biomedical Applications of Light Scattering IX, edited by Adam Wax, Vadim Backman, Proc. of SPIE
Vol. 9333, 93330Z · © 2015 SPIE · CCC code: 1605-7422/15/$18 · doi: 10.1117/12.2078027

sparsity of the submicron features and polarization of scattered light, we have been able to characterize human scalp hair with 20× objective at highly oblique LED illumination. Our method computes the distribution quality and area ratio of these features and, based on these numbers, can categorize black, blond, and grey hair into healthy and unhealthy (or damaged) with 100% success in our sample sets. This paves the way for lower cost, portable form factors such as cell phone add-ons[11] that could analyze hair quality.

2. EXPERIMENTAL SETUP

The setup consists of an infinity corrected objective (20× Olympus UPLSAPO Objective, 0.75NA, 0.6 mm WD) that is coupled into an aperture, a rotatable linear polarizer, and then a 1.3 mega pixel camera (Point grey FL3-U3-32S2C-CS). A hair strand is held vertically in midair with a sample holder and illuminated with a broadband non-polarized LED in highly oblique angle (85°) as in Fig. 2. The sample holder is coupled into a course 0.5" miniature dovetail mechanical 3D stage. The setup is not highly alignment sensitive due to low magnification.

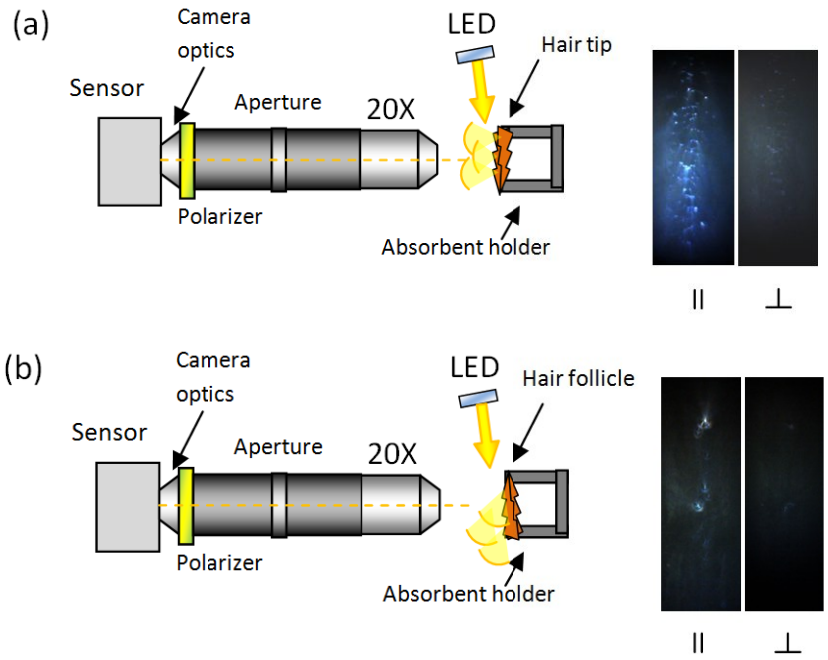

Figure 2. Measurement setup schematics. (a) Illumination from the tip side results in large number of spot-like features that can be detected with 20× objective. The scattering from the edges of the peeled cuticles is highly polarized as seen in the measurements on the right. (b) Illumination of the same sample from the follicle side. Only a few larger irregularities can be seen. (⊥ is cross polarized with cuticle scattering, ‖ is parallel polarization with these scatterings).

Due to specific geometry of hair, the difference between healthy and damaged hair becomes significantly evident (up to 8.5 times in the defined damage level parameter) when a hair strand is illuminated from the tip side. This is because there are more number of cuticles that are peeled off from the hair strand. The edges of these cuticles will scatter light that is strongly polarized in the horizontal direction compared to the weaker reflection from the body of the hair strand (Fig. 2 (a)). This helps us to record the background when the polarizer is cross polarized with the scattering from the cuticle edges (shown with ⊥ in Fig. 2). We realized that the background measurement was only necessary for grey hair when the reflection from the body of the hair is comparable with the cuticle edges. We also didn't find as significant scattering when we illuminated the sample with the same angle from the root side. This is expected as the peelings have small angle with the main axis of the hair strand (Fig. 2 (b)).

3. COMPUTATIONAL CATEGORIZATION

The block diagram of the computational categorization is shown in Fig. 3. The hair quality is categorized based on its color. If the hair is black or blonde, the algorithm extracts the features in the image and proceeds with the analysis. If the hair is grey, a preprocessing step is required to pronounce the features. For the grey hair the background is recorded when the scattered light from the cuticle edges are blocked by the polarizer. This background image is then subtracted after image registration (there is a small shift in the image when the polarization is rotated and this is compensated by image registration[12]). Although hair color can be easily distinguished under the microscope, we assume that it is an input from the user in this case.

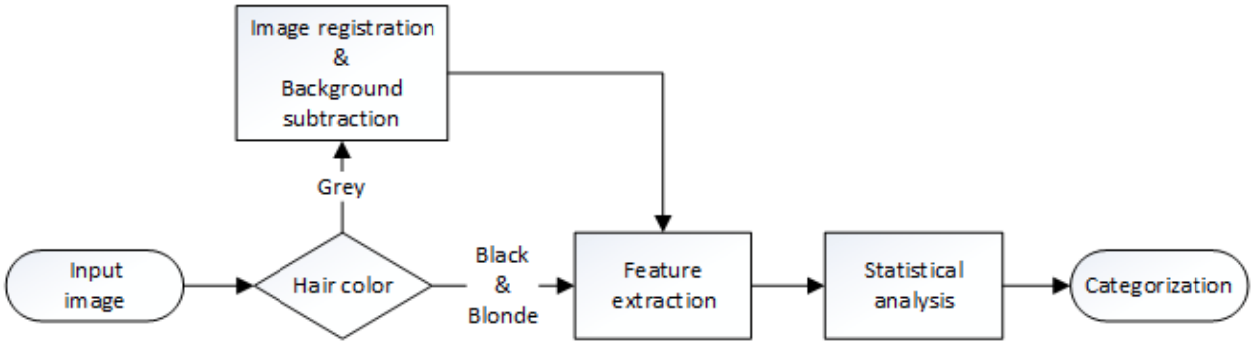

Figure 3. Block diagram of computational categorization process. Original red-green-blue (RGB) images are converted to grayscale as input image.

Features are extracted by using blob detection. This uses the regional maxima that are computed with a threshold, e.g, if blob intensity is over certain threshold, it is considered as a feature. To remove big or small blobs, the pixels in the region are filtered by using area criteria or number of pixels that are above the threshold in that region. After the features are extracted, the algorithm enters the statistical analysis block that consists of calculating distribution quality (DQ) and feature area ratio (FAR). The distribution quality of scattering features can be studied by using Delaunay triangles[13]. Another approach[12] was to find area ratio which contains features along each small image patch. We adapt this concept to measure the damage level of the hair.

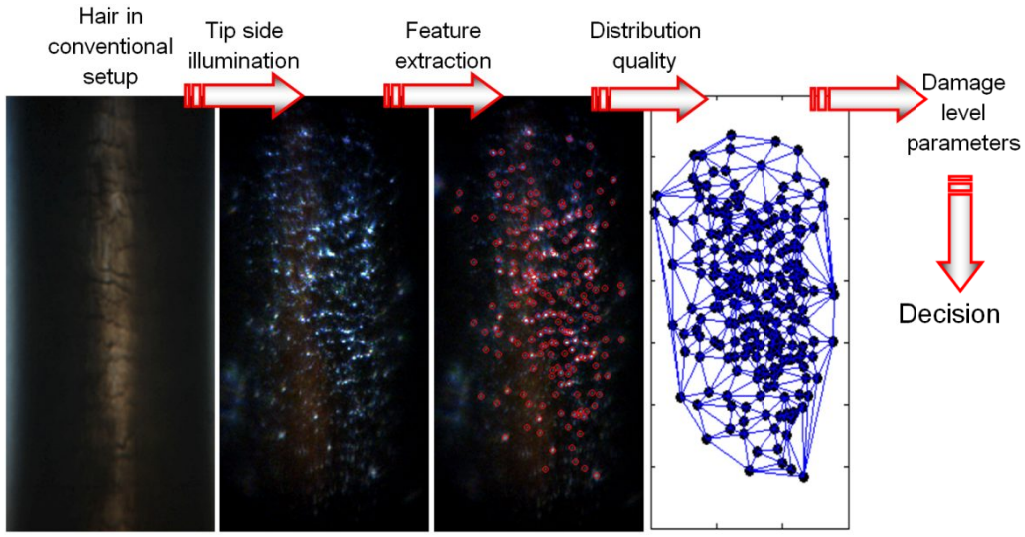

Figure 4. An example of our method applied to a real image that follows Fig. 3

To calculate FAR, a region of interest is selected as a mask. Then, region of interest (ROI) is divided into small image patches. If a feature existed in the patch, feature count is set to 1. This count is accumulated until last image patch is counted. Finally, FAR is calculated by using this accumulated counts over total number of patches. For example, if the size of ROI is 300×700 and the size of patch is 20×20, then we have (300/20)×(700/20) = 525 patches. If there are features on 75 patches, then FAR is 75/525 = 0.143.

For DQ the extracted features are considered as vertices of Delaunay triangles. The number of Delaunay triangles, the area of each triangle, and the radian value of each triangle contributes to the DQ.

Higher value of DQ and FAR depicts a higher damage level. To classify hair condition, these two parameters are simply multiplied to represent the damage level parameter. If this parameter is higher than certain level then the hair is categorized as damaged and vice versa. Fig. 4 shows an examples of an image that goes through this process: the highly oblique illumination intensifies the submicron features compared to conventional transmission or reflection imaging configuration with coaxial illumination; the features are extracted by blob detection as highlighted by red circles, the distribution quality and area ratio of these features are then calculated and multiplied to calculate the final damage level parameter. Finally the damage level is compared with a threshold to categorize the hair.

4. EXPERIMENTAL RESULTS

Our data sets are limited to black, blonde, and grey human scalp hair for this initial study. Each hair color data set consists of six images with three healthy and three damaged (96 hours UV exposed) hair images. As in Fig. 5 the highly oblique illumination from tip side of the hair renders healthy and damaged hair notably different.

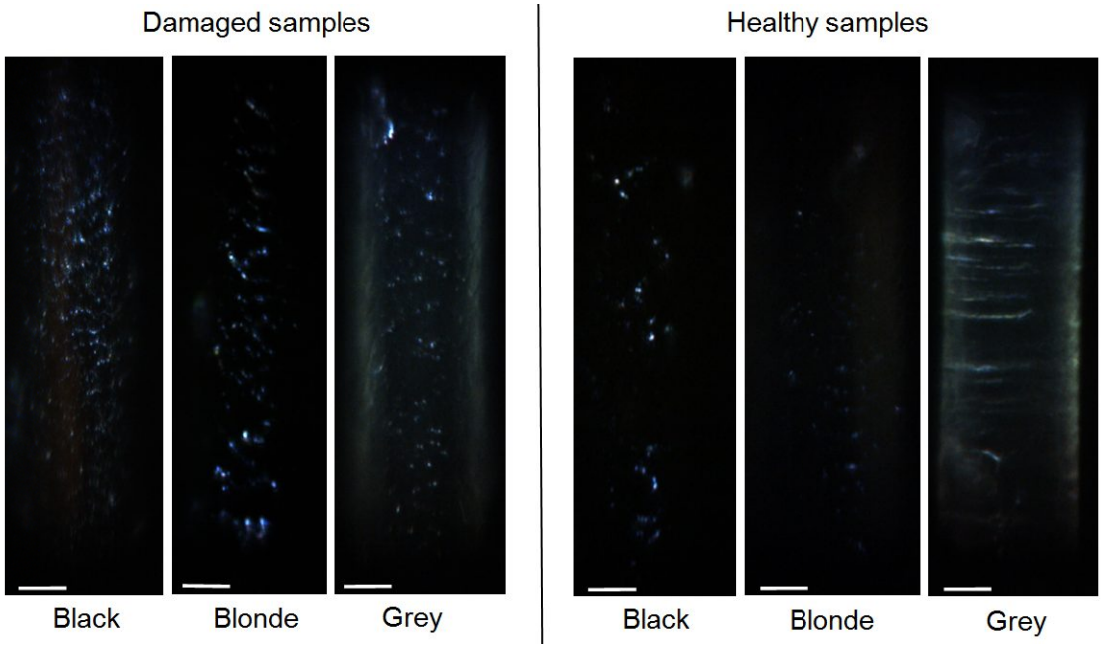

Figure 5. Healthy hair versus damaged hair (96 hours UV exposure). scale bar is 40 micrometer.

It is noteworthy that the imaged features are sparse and also not fully resolved as seen in Fig. 5. Therefore, the diffraction limit is not violated in any way. However, due to sparsity we can study the statistics of these and, therefore, categorize the hair as in Fig. 6. For all of our measurements we could find a threshold line in damage level parameter space that correctly categorized the samples into healthy and damaged as in Fig. 6. Fig. 6 (a) shows the calculated damage level for each hair color data set. As it is evident from this figure and also Fig. 5, the contrast between healthy and damaged hair is reduced as we go from black hair to grey hair. In this graph the decision line is drawn right between the boundary of healthy and damaged clusters. We expect to see some outliers as the number of samples are increased. However even in the current limited data set it is apparent that the data points start to form clusters above and below the decision line. Fig. 6 (b) shows further details of this decision lines which take the form of constant damage level curves; the clustering is also further evident here. It is noteworthy that the fixed damage level curves are just a simple and global categorization method that we have chosen and this might not necessarily be the best way to categorize these samples. A better decision making can be performed by molding this problem into an optimization framework.

As shown here lower magnifications can be used for categorizing different levels of hair damage. At this point we were unable to resolve the damage features properly with lower end 10X (0.25NA) objective. However, it is conceivable that if more than one strand of hair is used[2] or if higher resolution sensors (as in modern smartphones) are used there can be a better SNR for feature extraction. Another appealing direction can be use of laser illumination and very sensitive sensor that only measures the absolute value of scattering from the whole sample, this might sound as a simpler approach but regardless of accuracy it is relatively incompatible with today's portable electronic trends[11].

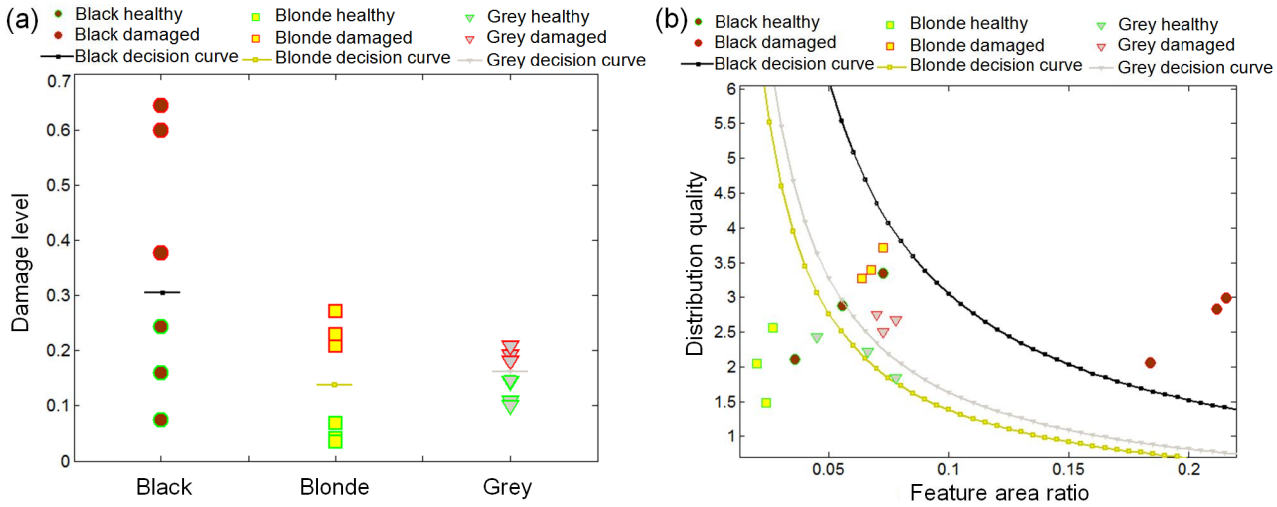

Figure 5.(a) different hair types are successfully categorized into healthy and unhealthy (a) Statistics of imaged features in high angle illuminations for healthy and unhealthy hair.

5. CONCLUSIONS

We have proposed and demonstrated a microscopy technique that can be used to investigate hair quality in lower magnifications. While the damage features are not directly resolvable, the sparsity of these features has allowed us to do statistical study of each sample and correctly categorize hair quality to healthy and damaged. This technique is not optically or computationally expensive and, therefore, is highly appealing for portable form factors for other samples that have sparse anisotropic surface irregularities such as ones in skin and nail.

6. ACKNOWLEDGMENTS

We acknowledge the contributions from Olympus Corporation and Natura.

7. REFERENCES

[1] Brown, A. C., Belser, R. B., Crounse, R. G. and Wehr, R. F., "A congenital hair defect: trichoschisis with alternating birefringence and low sulfur content," J. Invest. Dermatol., 54, 496–509 (1970).
[2] Lefaudeux, N., Lechocinski, N., Clemenceau, P. and Breugnot S., "New luster formula for the characterization of hair tresses using polarization imaging," J. Cosmet. Sci., 60, 153–169 (2009).
[3] Gamez-Garcia, M. and Lu, Y., "Light interference phenomena produced by cuticle cells of human hair," J. Cosmet. Sci., 58, 269-282 (2007).
[4] Lefaudeux, N., Lechocinski, N., Clemenceau, P. and Breugnot, S., [Chemical and Physical Behavior of Human Hair] 5th ed, Springer, (2012).
[5] Tsugita, T. and Iwai, T., "Optical coherence tomography using images of hair structure and dyes penetrating into the hair," Skin Res. Technol. (2014).

[6] Hadjur, C., Daty, G., Madry, G. and Corcuff, P., "Cosmetic assessment of the human hair by confocal microscopy," Scanning, 24, 59–64 (2002).
[7] Kuzuhara, A., "Analysis of structural changes in permanent waved human hair using Raman spectroscopy," Biopolymers, 85, 274–283 (2007).
[8] Jachowicz, J. and McMullen, R. L., "Tryptophan fluorescence in hair-examination of contributing factors," J. Cosmet. Sci., 62, 291-304 (2011).
[9] Nogueira, A. C. S., Diceliob, L. E. and Joekes, I., "Perspective about photo-damage of human hair," Photochem. Photobiol. Sci., 5, 165-169 (2006).
[10] Mertz, J., [Introduction to Optical Microscopy], Boberts & Company (2010).
[11] Zhu, H., Isikman, S. O., Mudanyali, O., Greenbaum, A. and Ozcan A., "Optical imaging techniques for point-of-care diagnostics," Lab Chip, 13, 51-67 (2013).
[12] Ik-Hyun, L. and Choi, T., "Accurate registration using adaptive block processing for multispectral images," IEEE Trans. Circuits Syst. Video Technol., 23, 1491-1501 (2013).
[13] Qing, Z., Wu, B. and Xu, Z., "Seed point selection method for triangle constrained image matching propagation," IEEE Geosci. Remote Sens. Lett., 3, 207-211 (2006).